Received: 16 January 2024 | Revised: 16 April 2024 | Accepted: 17 April 2024

DOI: 10.1111/gcb.17309

Global Change Biology WILEY

RESEARCH ARTICLE

Global evidence for joint effects of multiple natural and anthropogenic drivers on soil nitrogen cycling

Yong Zhang[1] | Xiaoli Cheng[1] | Cesar Terrer[2] | Woo-Jung Choi[3] | Ji Chen[4] | Yiqi Luo[5] | Philippe Ciais[6]

[1]Ministry of Education Key Laboratory for Transboundary Ecosecurity of Southwest China, School of Ecology and Environmental Science, Yunnan University, Kunming, China

[2]Department of Civil and Environmental Engineering, Massachusetts Institute of Technology, Cambridge, Massachusetts, USA

[3]Department of Rural & Bio-Systems Engineering, Chonnam National University, Gwangju, Republic of Korea

[4]State Key Laboratory of Loess and Quaternary Geology, Institute of Earth Environment, Chinese Academy of Sciences, Xi'an, China

[5]Soil and Crop Sciences Section, School of Integrative Plant Science, Cornell University, Ithaca, New York, USA

[6]Laboratoire des Sciences du Climat et de l'Environnement, Université Paris Saclay, Gif sur Yvette, France

Correspondence
Xiaoli Cheng, Ministry of Education Key Laboratory for Transboundary Ecosecurity of Southwest China, School of Ecology and Environmental Science, Yunnan University, Kunming, China.
Email: xlcheng@ynu.edu.cn

Funding information
H2020 Marie Skłodowska-Curie Actions, Grant/Award Number: 839806; National Natural Science Foundation of China, Grant/Award Number: 32130069; China National Scholarship, Grant/Award Number: BSY202309603

Abstract

Global soil nitrogen (N) cycling remains poorly understood due to its complex driving mechanisms. Here, we present a comprehensive analysis of global soil $\delta^{15}N$, a stable isotopic signature indicative of the N input–output balance, using a machine-learning approach on 10,676 observations from 2670 sites. Our findings reveal prevalent joint effects of climatic conditions, plant N-use strategies, soil properties, and other natural and anthropogenic forcings on global soil $\delta^{15}N$. The joint effects of multiple drivers govern the latitudinal distribution of soil $\delta^{15}N$, with more rapid N cycling at lower latitudes than at higher latitudes. In contrast to previous climate-focused models, our data-driven model more accurately simulates spatial changes in global soil $\delta^{15}N$, highlighting the need to consider the joint effects of multiple drivers to estimate the Earth's N budget. These insights contribute to the reconciliation of discordances among empirical, theoretical, and modeling studies on soil N cycling, as well as sustainable N management.

KEYWORDS
climatic conditions, natural and anthropogenic forcings, nitrogen isotope, plant traits, Rayleigh theory, soil properties

1 | INTRODUCTION

Soil nitrogen (N) cycling is a fundamental component of terrestrial biogeochemistry, yet the mechanisms controlling it remain unclear (Addiscott & Brookes, 2002; Hiltbrunner et al., 2019; Hungate et al., 2003; Olff et al., 2022). The stable N isotopic signature ($\delta^{15}N$) of soil reflects soil N input–output balance (Högberg, 1997; Robinson, 2001), where higher $\delta^{15}N$ values suggest a more open (leaky) N cycling and lower $\delta^{15}N$ values indicate a more close (conservative) N cycling (Mason et al., 2022; Peters et al., 2019). Microbial and enzymatic activities, which depend on temperature and moisture (Lohse et al., 2009), have long led researchers to expect that

climate (temperature and precipitation) predominantly controls soil $\delta^{15}N$ and N cycling, and some empirical evidence supports this notion (Amundson et al., 2003; Craine et al., 2015; Houlton et al., 2015; Houlton & Bai, 2009; Martinelli et al., 1999). However, climate-driven models based on such empirical evidence only account for a limited portion of the observed variation in global soil $\delta^{15}N$ (Amundson et al., 2003; Craine et al., 2015; Harris et al., 2022; Houlton et al., 2015; Houlton & Bai, 2009).

Alternative theoretical frameworks propose that soil N cycling is not solely controlled by climate, but rather is influenced by the joint effects of multiple drivers (climate, plant, soil, and others). Examples of these frameworks include isotope models (Brenner et al., 2001; Denk et al., 2019), the atmosphere–plant–soil continuum (Agren & Andersson, 2011; Brüggemann et al., 2011), and plant–soil-microbial feedbacks (Dawson et al., 2002; Hobbie, 2015). Soil $\delta^{15}N$ can be derived from mass balance models (Brenner et al., 2001; Robinson, 2001), state factor models (Amundson & Jenny, 1997), and kinetics models (Agren & Bosatta, 1998; Robinson, 2001) as described below:

$$\begin{cases} \delta_{soil}^{t+1} = f_{soil}^{t}\delta_{soil}^{t} + f_{input}^{t}\delta_{input}^{t} - f_{output}^{t}\delta_{output}^{t} \\ 1 = f_{soil}^{t} + f_{input}^{t} - f_{output}^{t} \\ d\left[f(t)\delta(t)\right]/dt = E(t)f(t)\delta(t), \end{cases} \quad (1)$$

where f and δ are the mass fraction and $\delta^{15}N$ value of the N-pool, respectively. $E(t)$ is the ecosystem operator (e.g., a wide range of natural and anthropogenic forcings) of the N-pool over time t. Input pools include N fertilization, N deposition, biological N-fixation, litter-N mineralization, and rock-N weathering. Output pools include plant N-uptake, leaching and gaseous N-losses. To date, the aforementioned theoretical frameworks have not been extensively tested by empirical studies.

The discrepancy among empirical, modeling, and theoretical studies (Agren & Andersson, 2011; Amundson et al., 2003; Bai, Houlton, et al., 2012; Brenner et al., 2001; Chen, Chen, et al., 2022; Craine et al., 2015; Denk et al., 2019; Harris et al., 2022; Houlton et al., 2015; Houlton & Bai, 2009; Robinson, 2001) suggests that the driving mechanisms of soil N cycling warrant further investigation. Here, we conducted a comprehensive analysis of global soil $\delta^{15}N$ using 10,676 observations from 2670 sites (Figure S1). The data were gathered through field surveys, dataset assembly and literature search, and then were standardized by the N isotope model and geographical aggregation. We also collected ancillary data as covariates from four categories (climate, plant, soil, and others; Table S1). The random-forest was identified as the most effective machine-learning algorithm and was used for variable importance analysis, variance partitioning, model simulation, and sensitivity analysis. Finally, we compared the performance of our model to that of climate-focused models. We aimed to explore: (i) the dominant drivers of global soil $\delta^{15}N$, (ii) how these dominant drivers shape spatial trends in global soil $\delta^{15}N$, and (iii) the implications for modeling global soil N cycling.

2 | METHODS

2.1 | Data compilation

2.1.1 | Field survey

A total of 410 soil samples were collected from 70 sites located in the Yangtze River basin between 2016 and 2021 (Figure S2), following standardized sampling protocol (Chen, Chen, et al., 2022). The dried soils were sieved (2-mm mesh) and finely grounded. Soil $\delta^{15}N$ was measured by an isotope ratio mass spectrometer (Flash HT2000, Thermo Fisher Scientific, Inc.) (Data S1).

2.1.2 | Dataset assembly

Three global datasets published between 2015 and 2022 (Choi et al., 2020; Craine et al., 2015; Harris et al., 2022) were included in our database after deduplication. Furthermore, we conducted extensive web-based searches for the datasets (~2022) recording soil $\delta^{15}N$ across Africa (Baumgartner et al., 2021; Carr et al., 2022; Mosher et al., 2020), America (Marty et al., 2019; Perakis et al., 2015; Sena-Souza et al., 2020), Asia (Hu et al., 2022; Shan et al., 2019), Europe (Guerrieri et al., 2021; Mullineaux et al., 2022; Thornton et al., 2015), and Oceania (Jones & Dalal, 2017; Rogers et al., 2022; Sommer et al., 2012). Based on the criterion described in the "Data standardization" section, 10188 observations were added to our database (Data S2).

2.1.3 | Literature search

We also conducted a search of published studies (~2022) reporting soil $\delta^{15}N$ in underrepresented regions, that is, Australia, Canada, Russia, India, desert and tundra biomes, tropical and polar zones. The keywords used in Web of Science were as follows: TS=("soil" AND "nitrogen") AND TS=("isotope" OR "15N") AND TS=("Australia" OR "Canada" OR "Russia" OR "India" OR "desert" OR "tundra" OR "tropical" OR "polar"). On the basis of the Preferred Reporting Items for Systematic Reviews and Meta-Analyses (PRISMA) protocols for literature search (Figure S3), 78 observations from 15 studies (Aaltonen et al., 2019; Bai, Sun, et al., 2012; Conradie et al., 2019; Ibell et al., 2013; Jung et al., 2013; Kellman et al., 2014; Kudrin et al., 2015; Makarov et al., 2008, 2019, 2021; Prokushkin et al., 2018; Semenyuk & Tiunov, 2011; Voronin et al., 2017; Wang et al., 2015; Ye et al., 2021) were supplemented (Data S3).

2.2 | Data standardization

2.2.1 | Soil $\delta^{15}N$

Observations should meet following requirements: (i) $\delta^{15}N$ values of total N in topsoil (<20 cm) under field conditions were measured;

(ii) geographic coordinates and ecosystem types (cropland, forest, grassland, open area, shrubland, or wetland) could be obtained; (iii) the measurements of $\delta^{15}N$ were within the accepted reference range ($-30‰ < \delta^{15}N < +30‰$) (Robinson, 2001); and (iv) observations were derived from non-manipulative experiments (e.g., without irrigation and warming).

The median year of soil sampling in our database was close to 2000 (Data S1–S3). To minimize the influence of sampling date, we simplified the soil N isotope model (Brenner et al., 2001; Sala et al., 2000) as a numerical function, $\delta(t)$, to normalize $\delta^{15}N$ observations to the year 2000:

$$\begin{cases} \delta(t) = \delta_0 + 0.081 \times t^{0.546} \\ \delta_{nor} = \delta_{obs} + \left[\delta\left(t_{age}\right) - \delta\left(t_{age} + t_{obs} - 2000\right)\right], \end{cases} \quad (2)$$

where t_{age} and t_{obs} are the soil age and the year of sampling, respectively; δ_{nor} and δ_{obs} are the normalized and observed $\delta^{15}N$ values, respectively. Soil ages were inferred from global radiocarbon measurements (Shi et al., 2020).

To reduce overrepresentation of specific locations, all normalized $\delta^{15}N$ values were aggregated by geographical distances (0.01°, ~1 km) and ecosystem types, denoted as site-averaged soil $\delta^{15}N$ (Craine et al., 2018; Sena-Souza et al., 2020). This aggregation also supported our exploration on the global pattern of soil $\delta^{15}N$ at the level of 1 km^2. Overall, 10,676 observations were aggregated into 2670 sites across different continents and climates (Figure S1). The subsequent analyses were based on site-averaged $\delta^{15}N$ data (Data S4).

2.2.2 | Covariates

To explore the dominant drivers and create spatially predictive models for global soil $\delta^{15}N$, 66 covariates (30-arcsecond resolution, ~1 km^2) were prepared following data assimilation approach (Cook-Patton et al., 2020). These covariates, derived from satellite-based remote sensing and ground-based field surveys, were summarized into four categories: climate (21 variables), plant (15 variables), soil (15 variables), and others (15 variables covering other natural and anthropogenic forcings). Please see detailed information on the 66 covariates in Table S1. To more realistically simulate global soil $\delta^{15}N$, we removed gridded data of the water, urban, and built-up areas.

2.3 | Algorithm selection

We compared four machine-learning algorithms generally used for ecology (Cook-Patton et al., 2020; Liang et al., 2022), that is, Random-Forest (RF) from R package *randomForest* (Breiman, 2001), eXtreme-Gradient-Boosting (XGB) from R package *xgboost* (Chen & Guestrin, 2016), Support-Vector-Machines (SVM) from R package *kernlab* (Karatzoglou et al., 2004), and Partial-Least-Squares (PLS) from R package *pls* (Mevik & Wehrens, 2007). Algorithm selections (hyperparameter optimization and cross-validation) were performed by the *expand. grid ()* function in the R base package and the *train ()* function in the R package *caret* (Kuhn, 2008). For each algorithm, a suite of hyperparameters was tested and then the best combination was selected. Please note that the RF algorithm selects a random subset of the features (i.e., feature bagging) at each candidate split in the learning process, thus can help avoid overfitting and multicollinearity (Breiman, 2001; Liang et al., 2022). We also used a feature selection algorithm to select the best subset of covariates for the XGB, SVM, and PLS algorithms, respectively, which can help mitigate overfitting risk and multicollinearity issue (Cook-Patton et al., 2020; Liang et al., 2022).

Random cross-validation was used to assess the performance of each algorithm in predicting soil $\delta^{15}N$. The full dataset was randomly separated into a training subset (90% of the data) and a testing subset (10%). A tenfold cross-validation with five replicates was used to determine the averages of root mean squared error (RMSE) and cross-validated R^2. We also used spatial cross-validation to evaluate the predictive power of each algorithm. The model trained by the training subset was scaled-up to create a global map, where we extracted the predicted $\delta^{15}N$. The predictive power was calculated as the R^2 between predicted and observed $\delta^{15}N$ for the testing subset. Random-forest algorithm was selected as the best one due to higher R^2 (Figures S4 and S5).

2.4 | Observational analysis

2.4.1 | Variable importance

Based on the full dataset, we assessed the relative importance of each covariate in explaining soil $\delta^{15}N$ by random-forest analysis (Breiman, 2001). The value of importance was calculated as mean increase in mean square error (%IncMSE). We used regression analysis to evaluate the difference among relative importances of the four categories of covariates. Difference is considered significant if $p < .05$. Note that variable importance is not for causal inference (Lucas, 2020; Yu et al., 2021).

2.4.2 | Variance partitioning

We repeated random-forest analyses with different input layers (i.e., different combinations of covariates): L_T, input layer with all covariates; L_1, input layer without climate variables; L_2, input layer without plant variables; L_3, input layer without soil variables; and L_4, input layer without other variables. The variance in soil $\delta^{15}N$ was partitioned into five components: I_T, the fraction explained by all covariates; I_1, the fraction jointly explained by plant, soil, and other variables; I_2, the fraction jointly explained by climate, soil, and other variables; I_3, the fraction jointly explained by climate, plant, and other variables; and I_4, the fraction jointly explained by climate, plant, and

soil variables. Thus, $I_T - I_1$, $I_T - I_2$, $I_T - I_3$, and $I_T - I_4$ represent the fraction uniquely explained by climate, plant, soil, and other variables, respectively (Peres-Neto et al., 2006). The fraction of each component can be estimated by cross-validated R^2 (Liang et al., 2022).

2.4.3 | Correlations

We also tested the correlations between soil $\delta^{15}N$ and 66 covariates. Continuous and categorical variables were tested by Pearson correlation analysis and linear regression analysis, respectively. Correlation is considered significant if $p < .05$.

2.5 | Model simulation

2.5.1 | Global simulation

We employed the full dataset and the random-forest algorithm with optimized parameters to train the spatially predictive model of soil $\delta^{15}N$ using the R package *caret* (Kuhn, 2008). In the R package *car* (Fox & Weisberg, 2019), the spatially predictive model was then applied to simulate soil $\delta^{15}N$ based on global gridded data of the covariates. We repeated these two processes to produce an ensemble of 20 independent global maps, and averaged these maps to create a final global map of soil $\delta^{15}N$. Uncertainty of the simulation was computed as the standard deviation of these 20 maps (Cook-Patton et al., 2020). The model performance was evaluated by the R^2 between simulated and observed $\delta^{15}N$ for the full dataset.

2.5.2 | Model sensitivity

We mapped the dominant drivers of global soil $\delta^{15}N$ following model sensitivity analysis (Liang et al., 2022). (i) A full random-forest model (R_T) was trained to create a final map (M_T) of soil $\delta^{15}N$ in the "Global simulation" section. (ii) Similarly, four reduced random-forest models were trained: R_1, the model without climate variables (V_1); R_2, the model without plant variables (V_2); R_3, the model without soil variables (V_3); and R_4, the model without other variables (V_4). We used these models to create four final maps (M_1, M_2, M_3, and M_4), respectively. (iii) The relative sensitivity (S_i) of R_i was calculated as: $S_i = |M_T - M_i| \div M_T$, where $i = 1$, 2, 3, and 4. For a given pixel (j) of M_i, its relative sensitivity was $S_{(i,j)}$. (iv) If $S_{(1,j)}$, $S_{(2,j)}$, $S_{(3,j)}$, and $S_{(4,j)}$ were all <0.2, we considered that j was in a scenario of joint effects of multiple drivers on soil $\delta^{15}N$; otherwise, the dominant driver of j was the category (V_i) with the highest relative sensitivity.

2.5.3 | Climate-zone simulation

On the basis of absolute latitude, the full dataset was stratified into four subsets (Bruno et al., 2018): (a) tropical zone, ranging from 0° to 23.5° (site = 553); (b) subtropical zone, ranging from 23.5° to 40° (site = 1080); (c) temperate zone, ranging from 40° to 66.5° (site = 1002); (d) polar zone, ranging from 66.5° to 90° (site = 35). Within these subsets, we repeated the soil $\delta^{15}N$ simulation and model sensitivity analysis for each climate-zone.

2.6 | Model comparison

We estimated globally mean soil $\delta^{15}N$ by integrating pixel values from the final map (M_T; 30-arcsecond resolution) of global soil $\delta^{15}N$. Our estimate was then compared to that of early climate-focused models, including the Community Land Model (CLM4.0 & CLM4.5) (Houlton et al., 2015), an artificial neural network (ANN) model (Harris et al., 2022), and the Climate Regression Model (ClimR) (Amundson et al., 2003; Houlton & Bai, 2009). To more directly compare to the climate-only ClimR model, we built a new ClimR model using our data (newClimR).

The difference ($\Delta\delta^{15}N$) between simulations of newClimR and our model (i.e., R_T) was quantified by newClimR minus R_T. We analyzed the spatial distribution of global $\Delta\delta^{15}N$. Given that the analytical precision of $\delta^{15}N$ was routinely ±0.2‰ (Robinson, 2001), the difference was considered significant if the absolute $\Delta\delta^{15}N$ was higher than tenfold precision (i.e., 2‰). The map pixels of $\Delta\delta^{15}N > 2‰$ and $\Delta\delta^{15}N < -2‰$ were grouped into overestimated and underestimated regions, respectively.

3 | RESULTS AND DISCUSSION

3.1 | Joint effects of multiple drivers on global soil $\delta^{15}N$ and the underlying mechanisms

We observed similar importance of climate, plant, soil, and other variables in explaining global soil $\delta^{15}N$ ($p = .537$; Figure 1a; Table S2). The fraction of variance uniquely explained by each category of these variables was small (0.5%–1.9%), with no significant difference among them ($p = .343$; Figure 1b). The majority of the 66 covariates were correlated with soil $\delta^{15}N$ ($p < .05$; Figure 1c; Figure S6). Moreover, our model explained most of the variation in soil $\delta^{15}N$ at a global scale ($R^2 = .901$; Figure 2a; Figure S7) and across different climate zones ($R^2 = .648$–$.908$; Figures S8A–S11A). The joint effects of multiple drivers (climate, plant, soil, and others) on soil $\delta^{15}N$ were evident in 88.4% of the global area analyzed (Figure 2b), and this pattern persisted across individual climate zones (54.5%–96.3% area; Figures S8B–S11B).

Our results uncover widespread joint effects of multiple drivers on global soil $\delta^{15}N$, supporting the theoretical frameworks that include multiple drivers of soil N cycling (Agren & Andersson, 2011; Brenner et al., 2001; Brüggemann et al., 2011; Dawson et al., 2002; Denk et al., 2019; Hobbie, 2015). The joint effects could be attributed to the N input–output balance and its underlying drivers (Figure 3a). Soil $\delta^{15}N$ is influenced by N flows and fractionations

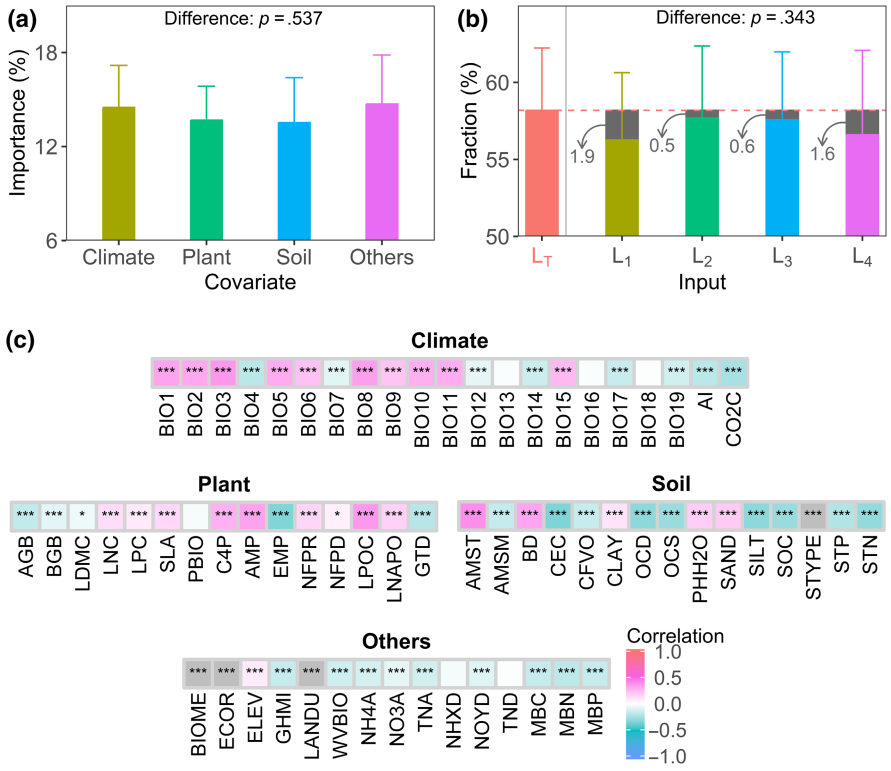

FIGURE 1 Observation of joint effects of multiple drivers on global soil $\delta^{15}N$. (a) Relative importance of the four categories of covariates in explaining $\delta^{15}N$. (b) The fraction of variance explained by different input layers. (c) Correlations between soil $\delta^{15}N$ and 66 covariates. L_T, input layer with all covariates; L_1, input layer without climate variables; L_2, input layer without plant variables; L_3, input layer without soil variables; and L_4, input layer without other variables. Please see detailed information on the 66 covariates in Table S1. Error bars indicate standard deviations. Gray cells indicate categorical variables. $^*p < .05$; $^{***}p < .001$.

within ecosystems (Högberg, 1997; Robinson, 2001). Drawing from global mean $\delta^{15}N$ across various pools (Figure 3a) and the Rayleigh theory (Rayleigh, 1896), we infer that organic N fertilization, plant N-uptake, rock-N weathering, and gaseous N-losses increase soil $\delta^{15}N$, whereas synthetic N fertilization, N deposition, biological N-fixation, and litter-N mineralization decrease it. This aligns with our findings that soil $\delta^{15}N$ increased with leaf N concentrations while it declined with synthetic N fertilization rates (Figure 1c; Figure S6). However, we also observed a positive correlation between soil $\delta^{15}N$ and factors including N-fixing plant richness and diversity (Figure 1c; Figure S6), which could be due to increased soil N losses (e.g., N_2O emission) via N-fixing plants (Kou-Giesbrecht & Menge, 2021). Consequently, shifts in soil $\delta^{15}N$ should account for both N inputs and outputs (Equation 1).

Furthermore, multiple drivers jointly control the N input–output balance in soils (Figure 3a). First, in terms of climate, faster soil N mineralization in hot/wet climates creates a greater proportion of gaseous N-losses (e.g., N_2O emission) and thus results in higher soil $\delta^{15}N$ (Amundson et al., 2003; Craine et al., 2015; Harris et al., 2022), as evidenced by our results (Figure 1c; Figure S6). Second, plants with flexible N-use strategies act as an important biotic factor, altering the N isotopic composition in soils (Evans, 2001; Robinson, 2001). In addition to the plant N-fixing capacity mentioned earlier, mycorrhizal associations also influence N isotope discrimination between plants and soils. Arbuscular mycorrhizal fungi are reported to aid inorganic N acquisition by plants (Govindarajulu et al., 2005), while ectomycorrhizal fungi can transfer organic N to plants (Lindahl & Tunlid, 2015). Given that organic N is more enriched in ^{15}N than inorganic N (Casciotti, 2016), arbuscular mycorrhizal and ectomycorrhizal fungi can cause higher and lower soil $\delta^{15}N$, respectively (Figure 1c; Figure S6). Third, soil properties typically reflect soil-forming processes (Agren & Andersson, 2011) and can affect soil $\delta^{15}N$. Most soil organic matter is plant-derived (Bird et al., 1996) and plants are ^{15}N-depleted relative to soils (Evans, 2001; Robinson, 2001), thus soil $\delta^{15}N$ decreases with increasing organic matter content (Figure 1c; Figure S6). Strong acid and alkaline soils have been shown to accelerate N_2O emission and NH_3 volatilization, respectively (Li et al., 2021; Zhang et al., 2022), which can enrich ^{15}N in soils (Figure 1c; Figure S6). Finally, other natural and anthropogenic forcings (e.g., N deposition, N fertilization, land-use types, etc.) may induce complex changes in soil $\delta^{15}N$ (Choi et al., 2020) (Figure 1c; Figure S6). For example, a recent study suggested that soil functions (e.g., mineralization) were jointly affected by multiple global change factors (Rillig et al., 2019).

3.2 | The joint effects of multiple drivers shape the latitudinal distribution of soil $\delta^{15}N$

Global soil $\delta^{15}N$ showed a latitudinal distribution with low-latitude regions (0°–40°; mean $\delta^{15}N = 6.059‰$) being ^{15}N-enriched relative to high-latitude regions (40°–80°; mean $\delta^{15}N = 2.910‰$), and there were widespread joint effects of multiple drivers on soil $\delta^{15}N$ across latitudinal gradients (Figure 3b,c). Low-latitude regions are often characterized by relatively hot/wet climates, widely distributed arbuscular mycorrhizal and N-fixing plants, low soil organic matter content, and intensive human activities;

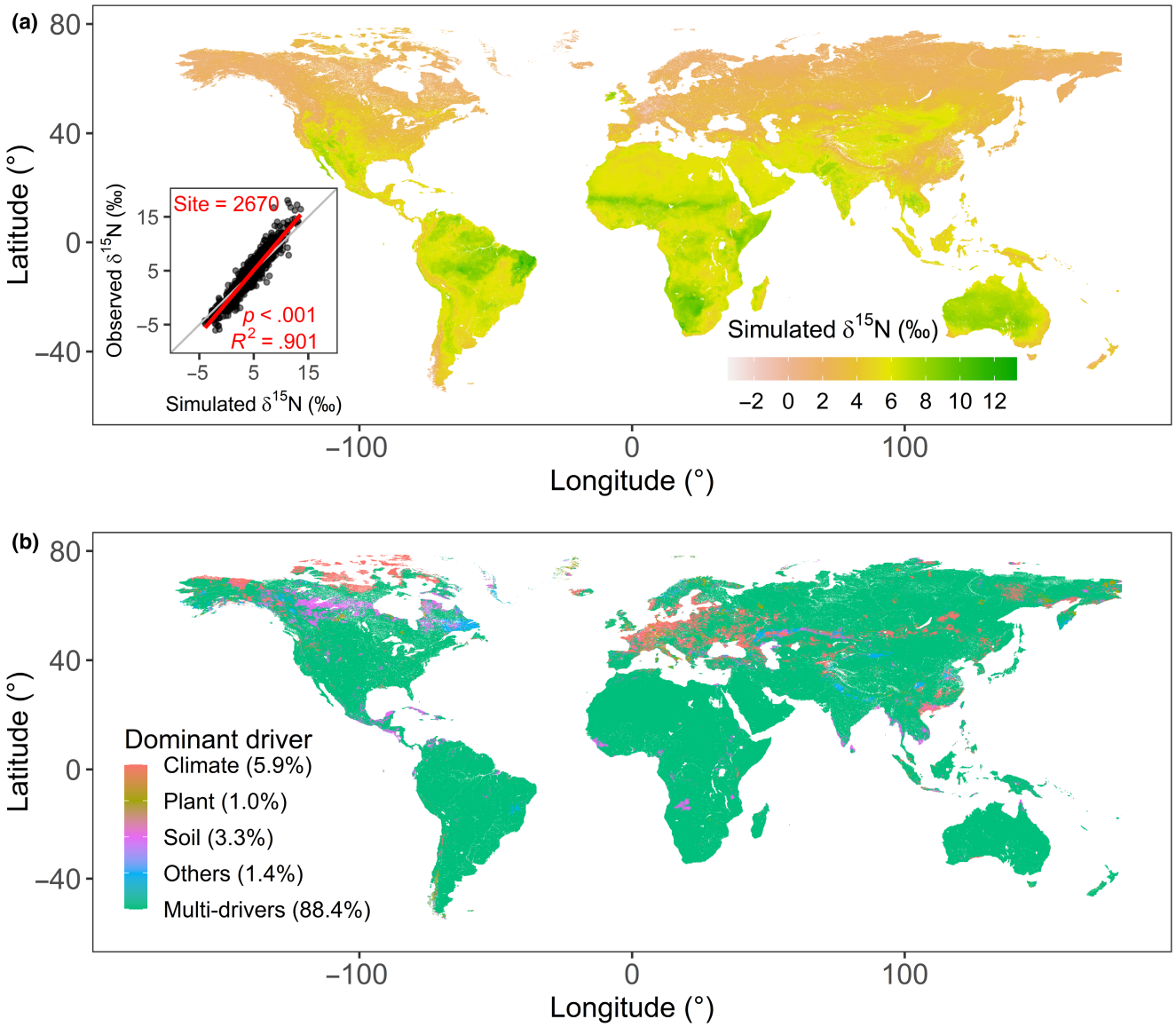

FIGURE 2 Simulation of joint effects of multiple drivers on global soil δ^{15}N. (a) Simulated soil δ^{15}N by the random-forest model. (b) Dominant drivers of global soil δ^{15}N. The "multi-drivers" term indicates a scenario of joint effects of multiple factors (climate, plant, soil, and others) on soil δ^{15}N. The number in parentheses indicates the percentage of each dominant driver in terms of area.

instead, high-latitude regions generally exhibit relatively cold/dry climates, widely distributed ectomycorrhizal plants, high soil organic matter content, and limited human activities (Fick & Hijmans, 2017; Poggio et al., 2021; Soudzilovskaia et al., 2019; Tamme et al., 2021; Theobald et al., 2020). These contrasting conditions lead to changes in soil δ^{15}N, indicating that the joint effects of multiple drivers shape the latitudinal distribution of soil δ^{15}N. Our explanations are further supported by the interactions between latitude and factors including mean annual temperature, mean annual precipitation, percentage of arbuscular mycorrhizal plants, percentage of ectomycorrhizal plants, N-fixing plant richness, N-fixing plant diversity, soil organic carbon content, land-use types, and N loading rates in affecting soil δ^{15}N ($p < .05$; Table S3).

3.3 | Implications for understanding and modeling global soil N cycling

In this study, we confirm the joint effects of multiple drivers on global soil N cycling, addressing the shortcomings of previous climate-driven hypotheses (Amundson et al., 2003; Craine et al., 2015; Houlton et al., 2015; Houlton & Bai, 2009; Martinelli et al., 1999) that underrepresent plant, soil, and other factors. This oversight can hinder the understanding of global soil N cycling and increase the uncertainties in global soil N cycle modeling (Chen et al., 2023). For example, our data-driven model estimated the mean δ^{15}N of global soils at 4.462‰ ($R^2 = .901$), while early climate-focused models, such as the Community Land Model

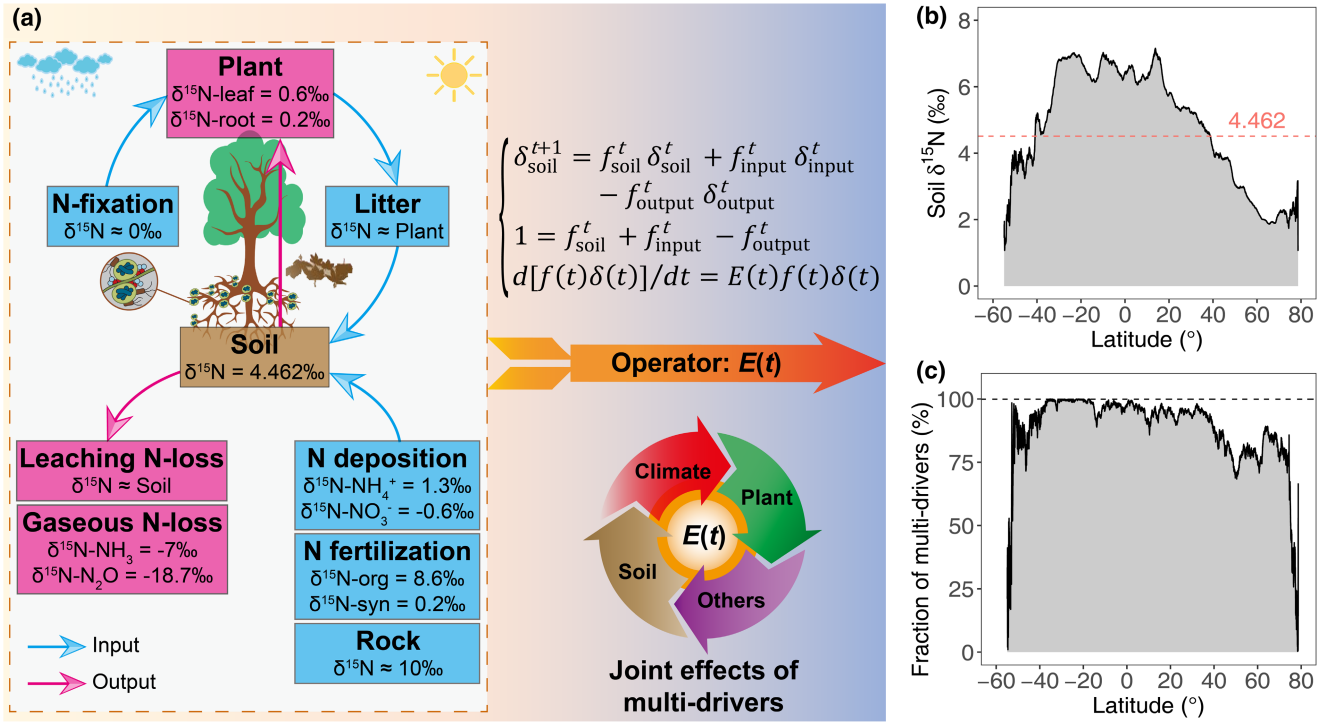

FIGURE 3 Mechanisms of joint effects of multiple drivers on global soil $\delta^{15}N$. (a) The input–output balance of global soil $\delta^{15}N$ and its underlying drivers. Latitudinal distributions for (b) soil $\delta^{15}N$ and (c) fraction of multi-drivers. The "multi-drivers" term indicates a scenario of joint effects of multiple factors (climate, plant, soil, and others) on soil $\delta^{15}N$. Global mean $\delta^{15}N$ values of various N pools were summarized by the following references: Plant (Craine et al., 2018; Kattge et al., 2020); N-fixation, Litter, and Leaching N-losses (Hobbie, 2015; Robinson, 2001); N deposition and Gaseous N-losses (Chen, Song, et al., 2022; Harris et al., 2022; Song et al., 2021); and N fertilization (Bateman & Kelly, 2007; Choi et al., 2020); Rock (Holloway & Dahlgren, 2002).

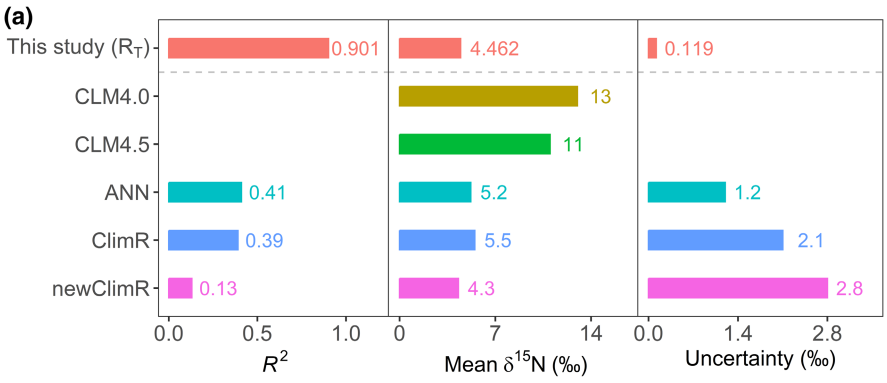

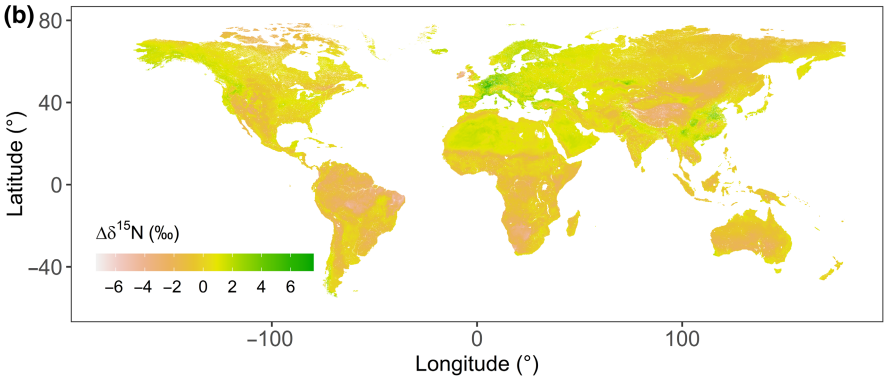

FIGURE 4 Model comparison. (a) Comparison of global estimates of soil $\delta^{15}N$ from different models. (b) Difference ($\Delta\delta^{15}N$) between soil $\delta^{15}N$ simulated by newClimR and this study. The uncertainties of R_T and ANN are expressed as standard deviations, and those of ClimR and newClimR as residual standard errors. ANN, artificial neural network model; ClimR, climate regression model; CLM, community land model; newClimR, ClimR model using our data; R_T, random-forest model.

(CLM4.0 and CLM4.5), an artificial neural network (ANN) model and the Climate Regression Model (ClimR), showed higher values (Figure 4a). Although the mean $\delta^{15}N$ estimated by the new ClimR model using our data (newClimR) was closer to our estimate, this model was very limited in explaining spatial changes of soil $\delta^{15}N$ ($R^2 = .130$), especially in the regions with weak or strong human modification (Figure 4b; Figure S12). These issues may be exacerbated in isotope models and Earth system models (Denk et al., 2019; Harris et al., 2022) when incorporating the products from climate-focused models, potentially having an adverse effect on the understanding and estimating of global N budget.

4 | CONCLUSIONS

In summary, our work highlights the joint effects of climatic conditions, plant N-use strategies, soil properties, and other natural and anthropogenic forcings on global soil $\delta^{15}N$, providing global evidence for the theoretical frameworks that include multiple drivers of soil N cycling (Agren & Andersson, 2011; Brenner et al., 2001; Brüggemann et al., 2011; Dawson et al., 2002; Denk et al., 2019; Hobbie, 2015). These insights should encourage efforts to reconcile the discrepancies among empirical, theoretical, and modeling studies on soil N cycling in complex ecosystems (Chen et al., 2023; Rillig et al., 2019). The Earth's N budget and sustainable N management would also benefit from a global framework of multiple drivers.

AUTHOR CONTRIBUTIONS

Yong Zhang: Conceptualization; data curation; formal analysis; methodology; validation; visualization; writing – original draft; writing – review and editing. **Xiaoli Cheng:** Conceptualization; data curation; formal analysis; funding acquisition; methodology; supervision; validation; visualization; writing – original draft; writing – review and editing. **Cesar Terrer:** Methodology; writing – review and editing. **Woo-Jung Choi:** Data curation; writing – review and editing. **Ji Chen:** Methodology; writing – review and editing. **Yiqi Luo:** Methodology; writing – review and editing. **Philippe Ciais:** Methodology; writing – review and editing.

ACKNOWLEDGMENTS

We thank the authors whose work was included in this study at the stage of dataset assembly and literature search, and the helps from Chang Liao, Qiong Chen, Dandan Zhang, Fan Yang, Qian Zhang, and Jiankun Bai at the stage of field survey. This study was funded by National Natural Science Foundation of China (32130069). Y.Z. received funding from China National Scholarship (BSY202309603). J.C. was funded by the EU H2020 Marie Sklodowska-Curie Actions (839806).

CONFLICT OF INTEREST STATEMENT

The authors declare no conflict of interest.

DATA AVAILABILITY STATEMENT

The data that support the findings of this study are openly available in Figshare at https://doi.org/10.6084/m9.figshare.23273945 (Zhang et al., 2024). Please see detailed information on the 66 covariates in Table S1.

ORCID

Yong Zhang https://orcid.org/0000-0002-1181-032X
Xiaoli Cheng https://orcid.org/0000-0002-0346-675X
Cesar Terrer https://orcid.org/0000-0002-5479-3486
Woo-Jung Choi https://orcid.org/0000-0002-2009-8207
Ji Chen https://orcid.org/0000-0001-7026-6312
Yiqi Luo https://orcid.org/0000-0002-4556-0218
Philippe Ciais https://orcid.org/0000-0001-8560-4943

REFERENCES

Aaltonen, H., Koster, K., Koster, E., Berninger, F., Zhou, X., Karhu, K., Biasi, C., Bruckman, V., Palviainen, M., & Pumpanen, J. (2019). Forest fires in Canadian permafrost region: The combined effects of fire and permafrost dynamics on soil organic matter quality. *Biogeochemistry*, *143*(2), 257–274. https://doi.org/10.1007/s10533-019-00560-x

Addiscott, T., & Brookes, P. (2002). What governs nitrogen loss from forest soils? *Nature*, *418*(6898), 604. https://doi.org/10.1038/418604a

Agren, G. I., & Andersson, F. O. (2011). *Terrestrial ecosystem ecology: Principles and applications*. Cambridge University Press.

Agren, G. I., & Bosatta, E. (1998). *Theoretical ecosystem ecology: Understanding element cycles*. Cambridge University Press.

Amundson, R., Austin, A. T., Schuur, E. A. G., Yoo, K., Matzek, V., Kendall, C., Uebersax, A., Brenner, D., & Baisden, W. T. (2003). Global patterns of the isotopic composition of soil and plant nitrogen. *Global Biogeochemical Cycles*, *17*(1), 1031. https://doi.org/10.1029/2002gb001903

Amundson, R., & Jenny, H. (1997). On a state factor model of ecosystems. *BioScience*, *47*(8), 536–543. https://doi.org/10.2307/1313122

Bai, E., Houlton, B. Z., & Wang, Y. P. (2012). Isotopic identification of nitrogen hotspots across natural terrestrial ecosystems. *Biogeosciences*, *9*(8), 3287–3304. https://doi.org/10.5194/bg-9-3287-2012

Bai, S. H., Sun, F., Xu, Z., Blumfield, T. J., Chen, C., & Wild, C. (2012). Appraisal of ^{15}N enrichment and ^{15}N natural abundance methods for estimating N_2 fixation by understorey *Acacia leiocalyx* and *A. disparimma* in a native forest of subtropical Australia. *Journal of Soils and Sediments*, *12*(5), 653–662. https://doi.org/10.1007/s11368-012-0492-2

Bateman, A. S., & Kelly, S. D. (2007). Fertilizer nitrogen isotope signatures. *Isotopes in Environmental and Health Studies*, *43*(3), 237–247. https://doi.org/10.1080/10256010701550732

Baumgartner, S., Bauters, M., Barthel, M., Drake, T. W., Ntaboba, L. C., Bazirake, B. M., Six, J., Boeckx, P., & Van Oost, K. (2021). Stable isotope signatures of soil nitrogen on an environmental–geomorphic gradient within The Congo Basin. *The Soil*, *7*(1), 83–94. https://doi.org/10.5194/soil-7-83-2021

Bird, M. I., Chivas, A. R., & Head, J. (1996). A latitudinal gradient in carbon turnover times in forest soils. *Nature*, *381*(6578), 143–146. https://doi.org/10.1038/381143a0

Breiman, L. (2001). Random forests. *Machine Learning*, *45*(1), 5–32. https://doi.org/10.1023/A:1010933404324

Brenner, D. L., Amundson, R., Baisden, W. T., Kendall, C., & Harden, J. (2001). Soil N and ^{15}N variation with time in a California annual

grassland ecosystem. *Geochimica et Cosmochimica Acta*, *65*(22), 4171–4186. https://doi.org/10.1016/S0016-7037(01)00699-8

Brüggemann, N., Gessler, A., Kayler, Z., Keel, S., Badeck, F., Barthel, M., Boeckx, P., Buchmann, N., Brugnoli, E., & Esperschütz, J. (2011). Carbon allocation and carbon isotope fluxes in the plant-soil-atmosphere continuum: A review. *Biogeosciences*, *8*(11), 3457–3489. https://doi.org/10.5194/bg-8-3457-2011

Bruno, J. F., Bates, A. E., Cacciapaglia, C., Pike, E. P., Amstrup, S. C., van Hooidonk, R., Henson, S. A., & Aronson, R. B. (2018). Climate change threatens the world's marine protected areas. *Nature Climate Change*, *8*(6), 499–503. https://doi.org/10.1038/s41558-018-0149-2

Carr, A. S., Chase, B. M., Boom, A., Meadows, M. E., & Sanchez, J. M. (2022). Variability in soil and foliar stable carbon and nitrogen isotope compositions in the winter rainfall biomes of South Africa. *Journal of Arid Environments*, *200*, 104726. https://doi.org/10.1016/j.jaridenv.2022.104726

Casciotti, K. L. (2016). Nitrogen and oxygen isotopic studies of the marine nitrogen cycle. *Annual Review of Marine Science*, *8*(1), 379–407. https://doi.org/10.1146/annurev-marine-010213-135052

Chen, J., Zhang, Y., Kuzyakov, Y., Wang, D., & Olesen, J. E. (2023). Challenges in upscaling laboratory studies to ecosystems in soil microbiology research. *Global Change Biology*, *29*(3), 569–574. https://doi.org/10.1111/gcb.16537

Chen, Q., Chen, J., Andersen, M. N., & Cheng, X. (2022). Elevational shifts in foliar-soil δ^{15}N in the Hengduan Mountains and different potential mechanisms. *Global Change Biology*, *28*(18), 5480–5491. https://doi.org/10.1111/gcb.16306

Chen, T., & Guestrin, C. (2016). *Xgboost: A scalable tree boosting system*. Paper presented at the the 22nd ACM SIGKDD International Conference on Knowledge Discovery and Data Mining, San Francisco. https://doi.org/10.1145/2939672.2939785

Chen, Z.-L., Song, W., Hu, C.-C., Liu, X.-J., Chen, G.-Y., Walters, W. W., Michalski, G., Liu, C.-Q., Fowler, D., & Liu, X.-Y. (2022). Significant contributions of combustion-related sources to ammonia emissions. *Nature Communications*, *13*(1), 7710. https://doi.org/10.1038/s41467-022-35381-4

Choi, W.-J., Kwak, J.-H., Park, H.-J., In Yang, H., Park, S.-I., Xu, Z., Lee, S.-M., Lim, S.-S., & Chang, S. X. (2020). Land-use type, and land management and disturbance affect soil δ^{15}N: A review. *Journal of Soils and Sediments*, *20*(9), 3283–3299. https://doi.org/10.1007/s11368-020-02708-x

Conradie, S. R., Hall, G., Somers, M. J., & McIntyre, T. (2019). Limited animal-facilitated nutrient transfer across an aquatic-terrestrial interface in a southern African savanna. *African Journal of Wildlife Research*, *49*(1), 52–61. https://doi.org/10.3957/056.049.0052

Cook-Patton, S. C., Leavitt, S. M., Gibbs, D., Harris, N. L., Lister, K., Anderson-Teixeira, K. J., Briggs, R. D., Chazdon, R. L., Crowther, T. W., Ellis, P. W., Griscom, H. P., Herrmann, V., Holl, K. D., Houghton, R. A., Larrosa, C., Lomax, G., Lucas, R., Madsen, P., Malhi, Y., … Griscom, B. W. (2020). Mapping carbon accumulation potential from global natural forest regrowth. *Nature*, *585*(7826), 545–550. https://doi.org/10.1038/s41586-020-2686-x

Craine, J. M., Elmore, A. J., Wang, L., Aranibar, J., Bauters, M., Boeckx, P., Crowley, B. E., Dawes, M. A., Delzon, S., Fajardo, A., Fang, Y., Fujiyoshi, L., Gray, A., Guerrieri, R., Gundale, M. J., Hawke, D. J., Hietz, P., Jonard, M., Kearsley, E., … Zmudczynska-Skarbek, K. (2018). Isotopic evidence for oligotrophication of terrestrial ecosystems. *Nature Ecology & Evolution*, *2*(11), 1735–1744. https://doi.org/10.1038/s41559-018-0694-0

Craine, J. M., Elmore, A. J., Wang, L., Augusto, L., Baisden, W. T., Brookshire, E. N. J., Cramer, M. D., Hasselquist, N. J., Hobbie, E. A., Kahmen, A., Koba, K., Kranabetter, J. M., Mack, M. C., Marin-Spiotta, E., Mayor, J. R., McLauchlan, K. K., Michelsen, A., Nardoto, G. B., Oliveira, R. S., … Zeller, B. (2015). Data from: Convergence of soil nitrogen isotopes across global climate gradients. *Dryad Digital Repository*, https://doi.org/10.5061/dryad.32ms0

Dawson, T. E., Mambelli, S., Plamboeck, A. H., Templer, P. H., & Tu, K. P. (2002). Stable isotopes in plant ecology. *Annual Review of Ecology and Systematics*, *33*(1), 507–559. https://doi.org/10.1146/annurev.ecolsys.33.020602.095451

Denk, T. R. A., Kraus, D., Kiese, R., Butterbach-Bahl, K., & Wolf, B. (2019). Constraining N cycling in the ecosystem model LandscapeDNDC with the stable isotope model SIMONE. *Ecology*, *100*(5), e02675. https://doi.org/10.1002/ecy.2675

Evans, R. D. (2001). Physiological mechanisms influencing plant nitrogen isotope composition. *Trends in Plant Science*, *6*(3), 121–126. https://doi.org/10.1016/S1360-1385(01)01889-1

Fick, S. E., & Hijmans, R. J. (2017). WorldClim 2: New 1-km spatial resolution climate surfaces for global land areas. *International Journal of Climatology*, *37*(12), 4302–4315. https://doi.org/10.1002/joc.5086

Fox, J., & Weisberg, S. (2019). *An R companion to applied regression*. SAGE Publications.

Govindarajulu, M., Pfeffer, P. E., Jin, H., Abubaker, J., Douds, D. D., Allen, J. W., Bücking, H., Lammers, P. J., & Shachar-Hill, Y. (2005). Nitrogen transfer in the arbuscular mycorrhizal symbiosis. *Nature*, *435*(7043), 819–823. https://doi.org/10.1038/nature03610

Guerrieri, R., Correia, M., Martín-Forés, I., Alfaro-Sánchez, R., Pino, J., Hampe, A., Valladares, F., & Espelta, J. M. (2021). Land-use legacies influence tree water-use efficiency and nitrogen availability in recently established European forests. *Functional Ecology*, *35*(6), 1325–1340. https://doi.org/10.1111/1365-2435.13787

Harris, E., Yu, L., Wang, Y. P., Mohn, J., Henne, S., Bai, E., Barthel, M., Bauters, M., Boeckx, P., Dorich, C., Farrell, M., Krummel, P. B., Loh, Z. M., Reichstein, M., Six, J., Steinbacher, M., Wells, N. S., Bahn, M., & Rayner, P. (2022). Data from: Warming and redistribution of nitrogen inputs drive an increase in terrestrial nitrous oxide emission factor. *Zenodo*, https://doi.org/10.5281/zenodo.6772207

Hiltbrunner, E., Körner, C., Meier, R., Braun, S., & Kahmen, A. (2019). Data do not support large-scale oligotrophication of terrestrial ecosystems. *Nature Ecology & Evolution*, *3*(9), 1285–1286. https://doi.org/10.1038/s41559-019-0948-5

Hobbie, S. E. (2015). Plant species effects on nutrient cycling: Revisiting litter feedbacks. *Trends in Ecology & Evolution*, *30*(6), 357–363. https://doi.org/10.1016/j.tree.2015.03.015

Högberg, P. (1997). ^{15}N natural abundance in soil-plant systems. *New Phytologist*, *137*(2), 179–203. https://doi.org/10.1046/j.1469-8137.1997.00808.x

Holloway, J. M., & Dahlgren, R. A. (2002). Nitrogen in rock: Occurrences and biogeochemical implications. *Global Biogeochemical Cycles*, *16*(4), 1118. https://doi.org/10.1029/2002GB001862

Houlton, B. Z., & Bai, E. (2009). Imprint of denitrifying bacteria on the global terrestrial biosphere. *Proceedings of the National Academy of Sciences of the United States of America*, *106*(51), 21713–21716. https://doi.org/10.1073/pnas.0912111106

Houlton, B. Z., Marklein, A. R., & Bai, E. (2015). Representation of nitrogen in climate change forecasts. *Nature Climate Change*, *5*(5), 398–401. https://doi.org/10.1038/nclimate2538

Hu, Y.-K., Liu, G.-F., Pan, X., Song, Y.-B., Dong, M., & Cornelissen, J. H. C. (2022). Contrasting nitrogen cycling between herbaceous wetland and terrestrial ecosystems inferred from plant and soil nitrogen isotopes across China. *Journal of Ecology*, *110*, 1259–1270. https://doi.org/10.1111/1365-2745.13866

Hungate, B. A., Dukes, J. S., Shaw, M. R., Luo, Y., & Field, C. B. (2003). Nitrogen and climate change. *Science*, *302*(5650), 1512–1513. https://doi.org/10.1126/science.1091390

Ibell, P. T., Xu, Z., & Blumfield, T. J. (2013). The influence of weed control on foliar δ^{15}N, δ^{13}C and tree growth in an 8 year-old exotic pine

plantation of subtropical Australia. *Plant and Soil*, *369*(1–2), 199–217. https://doi.org/10.1007/s11104-012-1554-3

Jones, A. R., & Dalal, R. C. (2017). Enrichment of natural ^{15}N abundance during soil N losses under 20 years of continuous cereal cropping. *Science of the Total Environment*, *574*, 282–287. https://doi.org/10.1016/j.scitotenv.2016.08.192

Jung, K., Choi, W.-J., Chang, S. X., & Arshad, M. A. (2013). Soil and tree ring chemistry of *Pinus banksiana* and *Populus tremuloides* stands as indicators of changes in atmospheric environments in the oil sands region of Alberta, Canada. *Ecological Indicators*, *25*, 256–265. https://doi.org/10.1016/j.ecolind.2012.10.006

Karatzoglou, A., Smola, A., Hornik, K., & Zeileis, A. (2004). *kernlab*—An S4 package for kernel methods in R. *Journal of Statistical Software*, *11*(9), 1–20. https://doi.org/10.18637/jss.v011.i09

Kattge, J., Bönisch, G., Díaz, S., Lavorel, S., Prentice, I. C., Leadley, P., Tautenhahn, S., Werner, G. D. A., Aakala, T., Abedi, M., Acosta, A. T. R., Adamidis, G. C., Adamson, K., Aiba, M., Albert, C. H., Alcántara, J. M., Alcázar, C. C., Aleixo, I., Ali, H., … Wirth, C. (2020). TRY plant trait database—Enhanced coverage and open access. *Global Change Biology*, *26*(1), 119–188. https://doi.org/10.1111/gcb.14904

Kellman, L., Kumar, S., & Diochon, A. (2014). Soil nitrogen dynamics within profiles of a managed moist temperate forest chronosequence consistent with long-term harvesting-induced losses. *Journal of Geophysical Research – Biogeosciences*, *119*(7), 1309–1321. https://doi.org/10.1002/2013jg002469

Kou-Giesbrecht, S., & Menge, D. N. L. (2021). Nitrogen-fixing trees increase soil nitrous oxide emissions: A meta-analysis. *Ecology*, *102*(8), e03415. https://doi.org/10.1002/ecy.3415

Kudrin, A. A., Tsurikov, S. M., & Tiunov, A. V. (2015). Trophic position of microbivorous and predatory soil nematodes in a boreal forest as indicated by stable isotope analysis. *Soil Biology & Biochemistry*, *86*, 193–200. https://doi.org/10.1016/j.soilbio.2015.03.017

Kuhn, M. (2008). Building predictive models in R using the *caret* package. *Journal of Statistical Software*, *28*(5), 1–26. https://doi.org/10.18637/jss.v028.i05

Li, C., Peng, F., Lai, C., Xue, X., You, Q., Chen, X., Liao, J., Ma, S., & Wang, T. (2021). Plant community changes determine the vegetation and soil $\delta^{13}C$ and $\delta^{15}N$ enrichment in degraded alpine grassland. *Land Degradation & Development*, *32*(7), 2371–2382. https://doi.org/10.1002/ldr.3912

Liang, J., Gamarra, J. G. P., Picard, N., Zhou, M., Pijanowski, B., Jacobs, D. F., Reich, P. B., Crowther, T. W., Nabuurs, G.-J., De-Miguel, S., Fang, J., Woodall, C. W., Svenning, J.-C., Jucker, T., Bastin, J.-F., Wiser, S. K., Slik, F., Hérault, B., Alberti, G., … Hui, C. (2022). Co-limitation towards lower latitudes shapes global forest diversity gradients. *Nature Ecology & Evolution*, *6*(10), 1423–1437. https://doi.org/10.1038/s41559-022-01831-x

Lindahl, B. D., & Tunlid, A. (2015). Ectomycorrhizal fungi—Potential organic matter decomposers, yet not saprotrophs. *New Phytologist*, *205*(4), 1443–1447. https://doi.org/10.1111/nph.13201

Lohse, K. A., Brooks, P. D., McIntosh, J. C., Meixner, T., & Huxman, T. E. (2009). Interactions between biogeochemistry and hydrologic systems. *Annual Review of Environment and Resources*, *34*(1), 65–96. https://doi.org/10.1146/annurev.environ.33.031207.111141

Lucas, T. C. D. (2020). A translucent box: Interpretable machine learning in ecology. *Ecological Monographs*, *90*(4), e01422. https://doi.org/10.1002/ecm.1422

Makarov, M. I., Kadulin, M. S., & Malysheva, T. I. (2021). ^{15}N natural abundance of soil microbial biomass in alpine and tundra ecosystems. *Eurasian Soil Science*, *54*(6), 907–917. https://doi.org/10.1134/s1064229321060107

Makarov, M. I., Malysheva, T. I., Cornelissen, J. H. C., van Logtestijn, R. S. P., & Glasser, B. (2008). Consistent patterns of ^{15}N distribution through soil profiles in diverse alpine and tundra ecosystems. *Soil Biology & Biochemistry*, *40*(5), 1082–1089. https://doi.org/10.1016/j.soilbio.2007.12.002

Makarov, M. I., Malysheva, T. I., & Menyailo, O. V. (2019). Isotopic composition of nitrogen and transformation of nitrogen compounds in meadow-alpine soils. *Eurasian Soil Science*, *52*(9), 1028–1037. https://doi.org/10.1134/s1064229319090059

Martinelli, L., Piccolo, M., Townsend, A., Vitousek, P., Cuevas, E., McDowell, W., Robertson, G., Santos, O., & Treseder, K. (1999). Nitrogen stable isotopic composition of leaves and soil: Tropical versus temperate forests. *Biogeochemistry*, *46*(1), 45–65. https://doi.org/10.1023/A:1006100128782

Marty, C., Houle, D., Courchesne, F., & Gagnon, C. (2019). Soil C:N ratio is the main driver of soil $\delta^{15}N$ in cold and N-limited eastern Canadian forests. *Catena*, *172*, 285–294. https://doi.org/10.1016/j.catena.2018.08.029

Mason, R. E., Craine, J. M., Lany, N. K., Jonard, M., Ollinger, S. V., Groffman, P. M., Fulweiler, R. W., Angerer, J., Read, Q. D., Reich, P. B., Templer, P. H., & Elmore, A. J. (2022). Evidence, causes, and consequences of declining nitrogen availability in terrestrial ecosystems. *Science*, *376*(6590), eabh3767. https://doi.org/10.1126/science.abh3767

Mevik, B.-H., & Wehrens, R. (2007). The *pls* package: Principal component and partial least squares regression in R. *Journal of Statistical Software*, *18*, 1–23. https://doi.org/10.18637/jss.v018.i02

Mosher, S. G., Crowley, B. E., Yanes, Y., Diefendorf, A. F., & Barone, R. (2020). Spatial variability in foliar carbon and nitrogen isotope values on Tenerife reflects both climate and soils: Establishing a framework for future work. *Acta Oecologica*, *109*, 103647. https://doi.org/10.1016/j.actao.2020.103647

Mullineaux, S. T., Kostka, B., Rock, L., Ogle, N., Marks, N. J., Doherty, R., Harrod, C., Montgomery, W. I., & Scantlebury, D. M. (2022). Soil $\delta^{13}C$ and $\delta^{15}N$ baselines clarify biogeographic heterogeneity in isotopic discrimination of European badgers (*Meles meles*). *Scientific Reports*, *12*(1), 200. https://doi.org/10.1038/s41598-021-04011-2

Olff, H., Aerts, R., Bobbink, R., Cornelissen, J. H. C., Erisman, J. W., Galloway, J. N., Stevens, C. J., Sutton, M. A., de Vries, F. T., Wamelink, G. W. W., & Wardle, D. A. (2022). Explanations for nitrogen decline. *Science*, *376*(6598), 1169–1170. https://doi.org/10.1126/science.abq7575

Perakis, S. S., Tepley, A. J., & Compton, J. E. (2015). Disturbance and topography shape nitrogen availability and $\delta^{15}N$ over long-term forest succession. *Ecosystems*, *18*(4), 573–588. https://doi.org/10.1007/s10021-015-9847-z

Peres-Neto, P. R., Legendre, P., Dray, S., & Borcard, D. (2006). Variation partitioning of species data matrices: Estimation and comparison of fractions. *Ecology*, *87*(10), 2614–2625. https://doi.org/10.1890/0012-9658(2006)87[2614:VPOSDM]2.0.CO;2

Peters, M. K., Hemp, A., Appelhans, T., Becker, J. N., Behler, C., Classen, A., Detsch, F., Ensslin, A., Ferger, S. W., Frederiksen, S. B., Gebert, F., Gerschlauer, F., Gutlein, A., Helbig-Bonitz, M., Hemp, C., Kindeketa, W. J., Kuhnel, A., Mayr, A. V., Mwangomo, E., … Steffan-Dewenter, I. (2019). Climate-land-use interactions shape tropical mountain biodiversity and ecosystem functions. *Nature*, *568*(7750), 88–92. https://doi.org/10.1038/s41586-019-1048-z

Poggio, L., De Sousa, L. M., Batjes, N. H., Heuvelink, G., Kempen, B., Ribeiro, E., & Rossiter, D. (2021). SoilGrids 2.0: Producing soil information for the globe with quantified spatial uncertainty. *The Soil*, *7*(1), 217–240. https://doi.org/10.5194/soil-2020-65

Prokushkin, A. S., Hagedorn, F., Pokrovsky, O. S., Viers, J., Kirdyanov, A. V., Masyagina, O. V., Prokushkina, M. P., & McDowell, W. H. (2018). Permafrost regime affects the nutritional status and productivity of larches in Central Siberia. *Forests*, *9*(6), 314. https://doi.org/10.3390/f9060314

Rayleigh, L. (1896). Theoretical considerations respecting the separation of gases by diffusion and similar processes. *Philosophical Magazine*, *42*(259), 493–498. https://doi.org/10.1080/14786449608620944

Rillig, M. C., Ryo, M., Lehmann, A., Aguilar-Trigueros, C. A., Buchert, S., Wulf, A., Iwasaki, A., Roy, J., & Yang, G. (2019). The role of multiple

global change factors in driving soil functions and microbial biodiversity. *Science*, *366*(6467), 886–890. https://doi.org/10.1126/science.aay2832

Robinson, D. (2001). δ^{15}N as an integrator of the nitrogen cycle. *Trends in Ecology & Evolution*, *16*(3), 153–162. https://doi.org/10.1016/S0169-5347(00)02098-X

Rogers, K. M., Martin, A. P., Pradel, G., Yuan, Y., Zhang, Y., & Turnbull, R. E. (2022). Elemental and isotopic compositions of New Zealand regional soils identifies human and climate-induced effects. *Applied Geochemistry*, *143*, 105356. https://doi.org/10.1016/j.apgeochem.2022.105356

Sala, O. E., Jackson, R. B., Mooney, H. A., & Howarth, R. W. (2000). *Methods in ecosystem science*. Springer Publishing Company.

Semenyuk, I. I., & Tiunov, A. V. (2011). Isotopic signature (^{15}N/^{14}N and ^{13}C/^{12}C) confirms similarity of trophic niches of millipedes (Myriapoda, Diplopoda) in a temperate deciduous forest. *Biology Bulletin*, *38*(3), 283–291. https://doi.org/10.1134/s1062359011030137

Sena-Souza, J. P., Houlton, B. Z., Martinelli, L. A., & Nardoto, G. B. (2020). Reconstructing continental-scale variation in soil δ^{15}N: A machine learning approach in South America. *Ecosphere*, *11*(8), e03223. https://doi.org/10.1002/ecs2.3223

Shan, Y., Huang, M., Suo, L., Zhao, X., & Wu, L. (2019). Composition and variation of soil δ^{15}N stable isotope in natural ecosystems. *Catena*, *183*, 104236. https://doi.org/10.1016/j.catena.2019.104236

Shi, Z., Allison, S. D., He, Y., Levine, P. A., Hoyt, A. M., Beem-Miller, J., Zhu, Q., Wieder, W. R., Trumbore, S., & Randerson, J. T. (2020). The age distribution of global soil carbon inferred from radiocarbon measurements. *Nature Geoscience*, *13*(8), 555–559. https://doi.org/10.1038/s41561-020-0596-z

Sommer, J., Pausch, J., Brundrett, M. C., Dixon, K. W., Bidartondo, M. I., & Gebauer, G. (2012). Limited carbon and mineral nutrient gain from mycorrhizal fungi by adult Australian orchids. *American Journal of Botany*, *99*(7), 1133–1145. https://doi.org/10.3732/ajb.1100575

Song, W., Liu, X.-Y., Hu, C.-C., Chen, G.-Y., Liu, X.-J., Walters, W. W., Michalski, G., & Liu, C.-Q. (2021). Important contributions of non-fossil fuel nitrogen oxides emissions. *Nature Communications*, *12*(1), 243. https://doi.org/10.1038/s41467-020-20356-0

Soudzilovskaia, N. A., van Bodegom, P. M., Terrer, C., Zelfde, M. V. T., McCallum, I., Luke McCormack, M., Fisher, J. B., Brundrett, M. C., De Sá, N. C., & Tedersoo, L. (2019). Global mycorrhizal plant distribution linked to terrestrial carbon stocks. *Nature Communications*, *10*(1), 5077. https://doi.org/10.1038/s41467-019-13019-2

Tamme, R., Pärtel, M., Kõljalg, U., Laanisto, L., Liira, J., Mander, Ü., Moora, M., Niinemets, Ü., Öpik, M., Ostonen, I., Tedersoo, L., & Zobel, M. (2021). Global macroecology of nitrogen-fixing plants. *Global Ecology and Biogeography*, *30*(2), 514–526. https://doi.org/10.1111/geb.13236

Theobald, D. M., Kennedy, C., Chen, B., Oakleaf, J., Baruch-Mordo, S., & Kiesecker, J. (2020). Earth transformed: Detailed mapping of global human modification from 1990 to 2017. *Earth System Science Data*, *12*(3), 1953–1972. https://doi.org/10.5194/essd-12-1953-2020

Thornton, B., Martin, G., Procee, M., Miller, D. R., Coull, M., Yao, H., Chapman, S. J., Hudson, G., & Midwood, A. J. (2015). Distributions of carbon and nitrogen isotopes in Scotland's topsoil: A national-scale study. *European Journal of Soil Science*, *66*(6), 1002–1011. https://doi.org/10.1111/ejss.12289

Voronin, P. Y., Mukhin, V. A., Velivetskaya, T. A., Ignat'ev, A. V., & Kuznetsov, V. V. (2017). Isotope composition of carbon and nitrogen in tissues and organs of *Betula pendula*. *Russian Journal of Plant Physiology*, *64*(2), 184–189. https://doi.org/10.1134/s1021443717010174

Wang, Y., Xu, Z., Zheng, J., Abdullah, K. M., & Zhou, Q. (2015). δ^{15}N of soil nitrogen pools and their dynamics under decomposing leaf litters in a suburban native forest subject to repeated prescribed burning in southeast Queensland, Australia. *Journal of Soils and Sediments*, *15*(5), 1063–1074. https://doi.org/10.1007/s11368-015-1117-3

Ye, L., Lata, J.-C., Nacro, H. B., Masse, D., & Barot, S. (2021). Effects of livestock on nitrogen and carbon cycling in a savanna in Burkina Faso. *Acta Oecologica*, *110*, 103694. https://doi.org/10.1016/j.actao.2020.103694

Yu, Q., Ji, W., Prihodko, L., Ross, C. W., Anchang, J. Y., & Hanan, N. P. (2021). Study becomes insight: Ecological learning from machine learning. *Methods in Ecology and Evolution*, *12*(11), 2117–2128. https://doi.org/10.1111/2041-210X.13686

Zhang, Y., Cheng, X., Terrer, C., Choi, W.-J., Chen, J., Luo, Y., & Ciais, P. (2024). Data from: Global evidence for joint effects of multiple natural and anthropogenic drivers on soil nitrogen cycling. *Figshare*, https://doi.org/10.6084/m9.figshare.23273945

Zhang, Y., Zhang, F., Abalos, D., Luo, Y., Hui, D., Hungate, B. A., García-Palacios, P., Kuzyakov, Y., Olesen, J. E., Jørgensen, U., & Chen, J. (2022). Stimulation of ammonia oxidizer and denitrifier abundances by nitrogen loading: Poor predictability for increased soil N_2O emission. *Global Change Biology*, *28*(6), 2158–2168. https://doi.org/10.1111/gcb.16042

SUPPORTING INFORMATION

Additional supporting information can be found online in the Supporting Information section at the end of this article.

How to cite this article: Zhang, Y., Cheng, X., Terrer, C., Choi, W.-J., Chen, J., Luo, Y., & Ciais, P. (2024). Global evidence for joint effects of multiple natural and anthropogenic drivers on soil nitrogen cycling. *Global Change Biology*, *30*, e17309. https://doi.org/10.1111/gcb.17309